A model of solar wind–magnetosphere–ionosphere coupling for due northward IMF

P. Song[a,*], T.I. Gombosi[a], D.L. DeZeeuw[a], K.G. Powell[b], C.P.T. Groth[a]

[a]*Space Physics Research Laboratory, Department of Atmospheric, Oceanic and Space Sciences, University of Michigan, 2455 Hayward Street, Ann Arbor, MI 48109-2143, USA*
[b]*W.M. Keck Foundation CFD Laboratory, Department of Aerospace Engineering, University of Michigan, Ann Arbor, MI 48109-2140, USA*

Abstract

A solar wind–magnetosphere–ionosphere coupling model for due northward IMF is proposed. The magnetosphere couples with the solar wind through reconnection nightside of the cusps. Other than the two small regions where reconnection takes place, the magnetosphere is closed. There are three plasma regions in the magnetosphere. The inner core is dominated by corotation. The outer magnetosphere contains two convection cells, and maps to the ionospheric viscous cells and Region I currents. The boundary layer and magnetotail region consists of a pair of flow channels, and maps to the ionospheric reverse cells. The three regions are separated by separatrix surfaces. Energy coupling across the surfaces can be facilitated by non-ideal-MHD processes such as ionospheric coupling, viscous and diffusive interactions, and waves and instabilities, although only the ionospheric coupling is essential to the model. This model is consistent with most established characteristics from observations and MHD computer simulations in both the ionosphere and magnetosphere. There are two specific features that need to be further confirmed from observations. The model expects that the ionospheric NBZ currents and reverse cells are maximized in the region sunward of the pole near the dayside cusps, and that in the tail there is a region which separates the earthward and tailward flows although the field and plasma characteristics are magnetospheric on both sides. © 1999 Elsevier Science Ltd. All rights reserved.

1. Introduction

Magnetospheric physics has entered a new era of global modeling. Pieces of understanding collected by various means from different regions are synthesized to gain the physical understanding of the global behavior of the terrestrial magnetosphere and its coupling to the solar wind and the ionosphere. However, there is an important piece of the global picture that is strikingly incomplete compared with other areas of progress. For a strongly northward interplanetary magnetic field (IMF), we presently lack a self-consistent global picture of magnetospheric and ionospheric convection patterns and the mapping between the two. In this paper, we report our attempt to address this question.

There are a number of major issues that have to be addressed in a solar wind–magnetosphere–ionosphere interaction model: (i) how is the solar wind mass, momentum and energy (including the Poynting flux) transferred into the magnetosphere; (ii) how is the low-latitude boundary layer (LLBL) formed if there is any; (iii) what is the global magnetospheric convection pattern; (iv) what is the ionospheric convection pattern that is consistent with the magnetospheric convection; (v) how is each region mapped in three dimensions in terms of magnetic field, electrical potential and electrical current, between the magnetosphere and the ionosphere?

For strongly northward IMF, it is widely agreed that the primary solar wind energy transfer mechanism is reconnection. Dungey (1961) first proposed the

* Corresponding author. Tel.: +1-734-764-8327; fax: +1-734-647-3083.

E-mail address: psong@engin.umich.edu (P. Song).

possibility of reconnection at the nightside of the cusps. In his model, the magnetosphere is closed. He discussed the topology in the noon–midnight meridian plane. The model we proposed in this paper is consistent with Dungey's original model in the noon–midnight plane and we provide the processes in three dimensions and coupling with the ionosphere. Kan and Burke (1985) proposed a global reconnection model for strongly northward IMF to explain the ionospheric convection patterns and theta aurora. Because their model involves a significant IMF B_x component and open magnetospheric field line regions embedded in the closed field regions, the global topology and geometry of the model is quite complicated. Song and Russell (1992) proposed a model of formation of the magnetospheric boundary layer through

cusp reconnection. Although their model is successful in explaining the observations of the low-latitude boundary layer and some cusp signatures, it does not describe the rest of the magnetosphere and the coupling with the ionosphere. Crooker (1992) provided a comprehensive review of the global models and ionospheric coupling for northward IMF and then proposed the concept of the over-draped lobe cells which corresponds to open field regions generated by reconnection between open magnetospheric lobe field lines and the IMF. The lobe cells are expected to be important when there is an IMF B_x component or a dipole tilt. Russell (1972), Reiff and Burch (1985), and Burch et al. (1992) proposed models for northward IMF when there is a significant IMF B_y component. These models involved cusp reconnection and lobe cells.
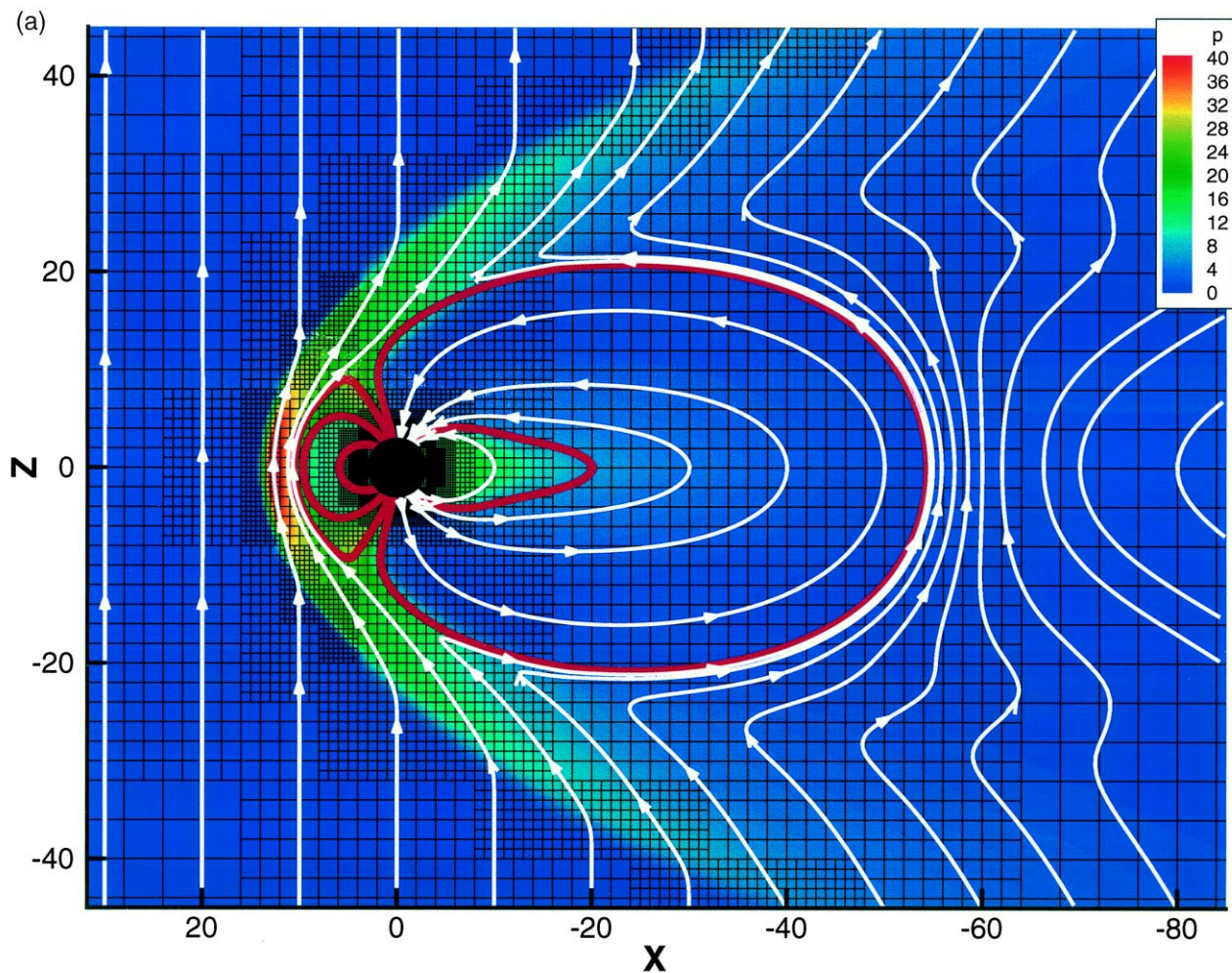

Fig. 1. Results of an MHD simulation for due northward IMF ($B_z = 5$ nT). (a) Noon–midnight meridian plane of the magnetosphere viewed from dusk. White lines are magnetic field lines. The thermal pressure distribution is color coded. The pressure increases downstream of the bow shock as the solar wind plasma is heated at the shock. Reconnection occurs in the nightside of the cusps. The thick red lines separate regions with distinct flow directions. (b) Northern ionosphere. The color coding shows the field-aligned current with red (blue) for currents flowing out of (into) the ionosphere, and the white lines show the convection pattern. The thick red lines mark the separation of different flow regions. The red dot sunward of the pole indicates the location of the mapping point between the footpoints of the two outmost red lines in (a). Points A and a in Fig. 2(c) are on each side of the center of the dot.
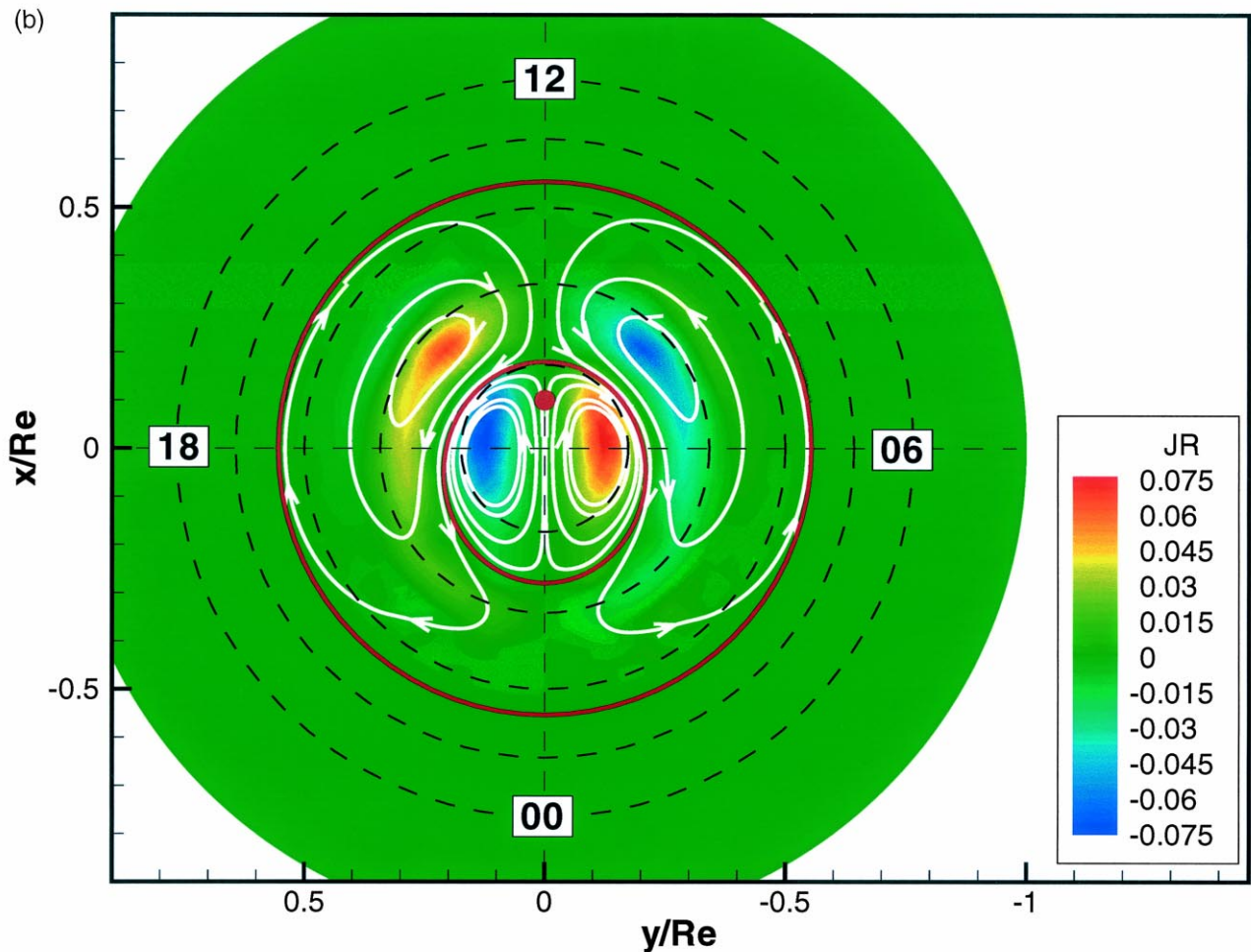
Fig. 1 (*continued*)

Compared with other aspects of our global understanding for northward IMF, the ionospheric convection pattern is relatively well established. In addition to the convection and field-aligned current systems for southward IMF, there is a pair of sunward convection cells and a pair of field-aligned currents at high latitudes (Burke et al., 1979; Iijima et al., 1984; Potemra et al., 1984; Clauer and Friis-Christensen, 1988; Taguchi and Hoffman, 1996). The two cells are usually referred to as the reverse cells and the field-aligned currents as the northward B_z (NBZ) Birkeland currents. Presently no model can explain these features and provide a three-dimensional (3-D) self-consistent picture of the whole system.

One of the main difficulties in modeling the magnetosphere for northward IMF arises from our poor understanding of whether the magnetosphere is closed or not. Most of magnetospheric in situ observations provide only local characteristics of the plasma and field properties. It is difficult to trace in three dimensions and globally map physical quantities reliably along streamlines and field lines. In contrast, on one hand, ionospheric observations provide better global diagnostics, even though with a lower spatial resolution. On the other hand, the topology of the magnetospheric field derived from the ionospheric observations depends highly on the models used in the interpretation. For example, in many models, the edge of the polar cap has been interpreted as the boundary between open and closed field lines because solar wind particles are seen within the polar cap. However, the precipitation along newly closed field lines through pitch angle diffusion can provide similar particle characteristics. Another example is the antisunward convection of viscous cells (these are a pair of ionospheric cells equatorward of the reverse cells), which has often been interpreted as the evidence for viscous interaction between the region of closed magnetospheric field lines and the solar wind, because antisunward plasma convection is in the same direction as the solar wind drag on the magnetospheric boundary layer. It follows from this argument that the reverse

cells should be on open field lines, and consequently, the NBZ currents should map to the solar wind because they are closely related to the reverse cells. However, so far no one has successfully shown how the solar wind can generate currents of such a polarity as the NBZ currents. Another difficulty is how to map the fields and currents globally in three dimensions. Previous models provide such mapping only in part of the system or in one or two cross-sections.

In addition to traditional qualitative theoretical modeling, global computer simulations provide a new way to understand the global behavior of the solar wind–magnetosphere–ionosphere system (e.g., Ogino and Walker, 1984; Wu, 1985; Usadi et al., 1993; Winglee, 1994; Fedder and Lyon, 1995; Berchem et al., 1995; Raeder et al., 1995; Gombosi et al., 1998). These simulations provide self-consistent solutions in a large region in the system. However, these solutions depend strongly on the boundary conditions and the numerical schemes used in the simulation. The results of a simulation need to be compared with theoretical models and observations for validation. The simulation results will be discussed throughout this paper when they are relevant. Discussion of the differences among these simulation models will be presented in detail in a separate paper. Even if a simulation model is valid, qualitative theoretical models remain to be important to provide the understanding of the key physical processes in the system, given that a simulation result is often complication by numerical noise and boundary effects.

2. Simulation

Fig. 1 shows an example of the simulation results for due northward IMF (Gombosi et al., 1998). In this simulation model, ideal-MHD equations are solved under an adaptive grid system. The size of the grids ranges from 1/8 Re near the Earth to 4 Re far from the Earth in the solar wind. The numerical algorithm used to solve the governing equations has three key ingredients. It is an upwind scheme in order to solve the hyperbolic system. It uses a Riemann solver that solves the eigen modes and their propagation in the system and provides robust solutions with low dissipation. It employs a limited reconstruction scheme which ensure solutions to second-order accuracy in the region away from discontinuities while providing the stability in the solutions.

The solutions at the inner boundary of the magnetospheric simulation at 3 Re in radius are mapped to the ionosphere at 400 km along a dipole field. Then the component of the field-aligned currents $J_\parallel$ normal to the ionospheric boundary is used as the source term in a two-dimensional (2-D) ionospheric electric potential equation. Namely,

$$\nabla_i \times (\Sigma \times \nabla_i \phi) = J_\parallel \ \sin \ \theta$$

where ϕ is the ionospheric electric potential, Σ is the height-integrated conductivity tensor, ∇_i is a 2-D ionospheric derivative operator, and θ is the angle between the magnetic field and the radial direction at the ionosphere. In the present run, we have assumed the ionospheric conductivity to be uniform and the Hall conductance to be zero. The resultant electric potential is mapped back to the inner boundary of the magnetospheric simulation. The electric field is derived by $\mathbf{E} = -\nabla\phi$, and the convection velocity is assumed to be the electric field drift velocity

$$\mathbf{V}_d = \mathbf{E} \times \mathbf{B}/B^2$$

The derived drift velocity is then used as the inner boundary condition for the magnetospheric simulation. The iteration between magnetospheric velocity $\mathbf{V}_m$ and $\mathbf{V}_d$ continues until they become the same.

The initial conditions for the present simulations are such that plasma parameters are the same as the solar wind conditions and the magnetic field is the superposition of an IMF with a dipole field. Different initial conditions have been tested. The resulting steady-state solutions are the same; indicating that the steady-state solution of the whole system is independent of the initial conditions (Gombosi et al., 1999).

The parameters used in the run shown in Fig. 1 are typical of solar wind: density 5/cc, velocity 400 km/s, thermal speed 50 km/s, sonic Mach number 8. The IMF is purely northward with a magnitude of 5 nT. The resulting solar wind Alfven velocity is 49 km/s and solar wind plasma beta is near $2/\gamma = 1.2$. The ionospheric conductance is uniformly 5 mhos.

As shown in Fig. 1(a), the bow shock is formed in front of the magnetosphere. It decelerates, deflects and heats the solar wind plasma. The magnetosphere is closed other than the two small regions near the cusps where reconnection takes place. Fig. 1(b) shows the results at the ionosphere. As shown by the color coding, there are three pairs of the field-aligned currents. From the high-latitude to low-latitude, they have the same polarity as the NBZ, Region I and II currents, respectively. Associated with the NBZ currents is a pair of sunward convection cells, in the same sense as the reverse cells. At the low-latitude side of the reverse cells is a pair of antisunward convection cells with the same sense as the viscous cells. Since the simulation model is based on ideal-MHD and does not represent the physical processes of Region II currents, we will not discuss the currents with Region II polarity.

In the present work, we use the numerical tools provided by MHD simulations to trace streamlines and map field lines globally, and hence, to understand the

3-D characteristics of the solar wind–magnetosphere–ionosphere coupling for due northward IMF. When we performed the field line mapping and streamline tracing in 3-D, we found that some results are different and others are missing in our conventional picture. The model described is based on the information obtained from the 3-D global mapping and tracing, previous observations, and required theoretical consistency. In the present model, we focus on qualitative global processes. We address the basic patterns of convection, currents and field configuration, and the global coupling mechanisms. We do not compare our model quantitatively with simulation results.

3. Theoretical model

3.1. Solar wind energy transfer

A fundamental assumption of our model, the same as Dungey's (1961) model and that shown in Fig. 1, is that mass, momentum and energy is coupled between the solar wind and the magnetosphere primarily via reconnection between the IMF and the magnetospheric field. Reconnection takes place in a region nightside of each cusp where the draped magnetosheath field is mostly antiparallel to the magnetospheric field. As discussed by Song and Russell (1992) and Song et al. (1994), reconnection occurs in a relatively small region in the y-direction because as y increases, the magnetosheath and magnetospheric fields become less antiparallel and the reconnection rate decreases. Exact width of the reconnection line will affect the total amount of the mass and energy transferred from the magnetosheath to the magnetosphere, and, however, is not critical to our model.

The reconnection process could take place in either steady-state (Dungey, 1961) or time dependent (Song and Russell, 1992) manner. If it is time dependent, the present model describes the time average of the global convection pattern. The reconnection process poleward of the cusps has been shown in all MHD simulations for northward IMF (e.g., Ogino and Walker, 1984; Wu, 1985; Usadi et al., 1993; Fedder and Lyon, 1995; Berchem et al., 1995; Raeder et al., 1995; Gombosi et al., 1999). It has also been observed in space (Gosling et al., 1991; Kessel et al., 1996) (also see a summary by Song and Russell, 1992). Furthermore, Feldman et al. (1995) reported evidence for conjugate reconnection.

Through the reconnection process at both ends, a solar wind flux tube is effectively captured by the magnetosphere with its solar wind plasma and motional electric field. This is the primary source of energy that drives the magnetospheric and ionospheric convection in our model. In the simulation shown in Fig. 1,

because a North–South symmetry has been assumed, reconnection at two hemispheres occurs on the same IMF flux tube simultaneously. It is worth mentioning that because of numerical errors in field line tracing techniques near reconnection regions, it is possible that reconnection in the two hemispheres appear to be on different IMF flux tubes although the numerical solution is North–South symmetric. In reality, the reconnection events at the two cusps do not need to take place simultaneously, as discussed by Song and Russell (1992) and Song et al. (1994). A timing difference between the two reconnection events on an IMF flux tube will reduce the built-up pressure to be discussed next. However, the basic processes remain qualitatively the same.

3.2. Formation of the LLBL

The newly captured solar wind flux tube contains fresh solar wind particles. When the flux tube 'sinks' into the magnetosphere as a result of the propagation, from the cusps to the equator, of the kinks where it threads the magnetopause (Song and Russell, 1992), it gets compressed, because the magnetospheric field is stronger than the sheath field. The reconnected flux tube is also shortened associated with the tension release near the cusp sunward of the reconnection regions as seen in Fig. 1(a). These two processes tend to build a higher pressure near the subsolar region. The high pressure can be held radially by the tension force of the newly formed magnetospheric flux tube, but the pressure gradient in the azimuthal direction will lead to an expansion of the flux tube. Required by the interchange instability condition, the expansion of the newly closed flux tube will be along the magnetopause similar to a 'coating' process and forms the LLBL. More detailed discussion on the formation of the LLBL can be found in Song and Russell (1992), Yang et al. (1994), and Song et al. (1994).

3.3. Topology

Fig. 2 shows a qualitative theoretical version of Fig. 1. Here we remark that our theoretical model is not necessarily identical to the simulation results because the simulation is limited by the numerical limitation, boundary conditions and physical processes included in the model. The magnetosphere is on closed field lines except a small region near point X on the nightside of each cusp where reconnection between the IMF and magnetospheric field lines takes place. A nearly closed magnetosphere was first conceived by Dungey (1961) and later shown in many global MHD simulations for northward IMF (e.g., Wu, 1985; Usadi et al., 1993; Fedder and Lyon, 1995; Gombosi et al., 1999). The absence of the open magnetotail during
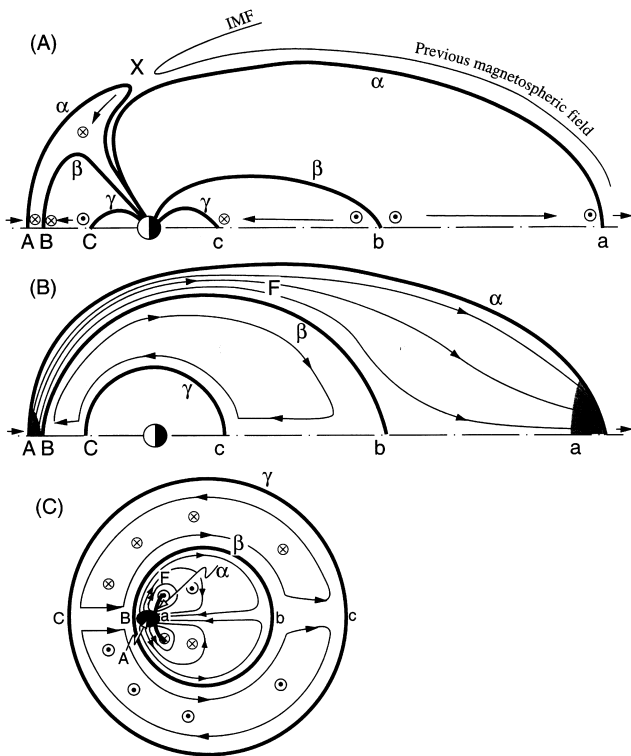
Fig. 2. Global geometry of the magnetosphere and ionospheric mapping. In all panels, thick solid lines represent the separatrix surfaces and thin solid lines with arrowheads indicate the direction of the flow, and the shaded areas indicate the regions ambient to newly reconnected/disconnected field lines and their topological status is ambiguous. (a) The noon–midnight meridian plane of the magnetosphere viewed from dusk. Circles with crosses (dots) indicate the plasma flows away from (toward) the reader. Surface α (the magnetopause/cusp) is the surface consisting of curves A–X–Earth in the dayside and Earth–a in the nightside. Surface β consists of curves B–Earth in the dayside and Earth–b in the nightside, and surface γ (plasmapause) consists of curves C–Earth and Earth–c. (b) The equatorial plane of the magnetosphere viewed from North. Point F indicates where the boundary layer streamline turns away from the Sun–Earth line to towards the Sun–Earth line, and maps to the ends of the cusp arc in panel c. (c) The northern ionosphere viewed from the top. The circles with dots and crosses indicate the directions of the field-aligned currents, instead of the plasma flows.

strongly northward IMF periods indicates a closed magnetosphere during northward IMF (Fairfield, 1993; Fairfield et al., 1996). As we discussed in the Introduction, the interpretations of some ionospheric observations as an indication of an open magnetosphere for northward IMF are debatable.

As a result of reconnection, the portion of the IMF flux tube dayside of point X is connected with the polar region magnetospheric fields to form a newly closed field line (filled with fresh solar wind plasma), and a significant portion of a tail field line (filled with magnetospheric plasma) is disconnected from the closed magnetotail as it 're-emerges' from the tail and is carried away by the solar wind. The topological status of the field lines near the reconnection points is

ambiguous because the dayside (nightside) field lines are newly reconnected (disconnected) and their particle characteristics are in transition from one status to the other. These regions are indicated by shaded areas in Fig. 2. As we stated earlier, the width of the area in the dawn–dusk direction is not critical to our model although it is important in determining quantitatively the amount of the mass and energy transferred.

In our model the magnetosphere is divided into three distinct plasma regions. As shown in Fig. 2, they are the inner core, the outer magnetosphere/near Earth tail region, and the boundary layer/distant tail region. The three regions are bounded by three separatrix surfaces (thick lines, α, β and γ) and the ionosphere. Surface α is defined by the separatrix surface between the magnetospheric field and the magnetosheath field. It is immediately outside of the surface formed by the last closed field lines. There is a hole on surface α at the reconnection site near each cusp. Surfaces β and γ are derived by tracing the streamlines in the equatorial plane. When tracing streamlines from the dayside to the nightside in the equatorial plane, one finds that near the magnetopause boundary, the streamlines go into the solar wind on the nightside. However, further inside the magnetosphere, the streamlines go to nightside and return back. There is a line on each side of which the two neighboring streamlines diverge at a certain point b at midnight. The line between these two streamlines is referred to as a separatrix. Mapping the separatrix along the field lines to the ionosphere forms a shell surface and is referred to as surface β. Similarly, the earthward flow from point b in the equatorial plane will diverge at a certain point c where the magnetic pressure becomes strong enough to stop further flowing. The line earthward of the last streamline and its mapping along the field forms surface γ.

Within each region, ideal-MHD may describe the dominant processes while non-ideal-MHD effects may play minor roles. Across the separatrix surfaces (in particular across the surface between the magnetosphere and boundary layer/tail, surface β), mass, momentum and energy can be transferred through ionospheric coupling and viscous and diffusive interactions. However, in our model, only the ionospheric coupling is critical in the coupling process. The other non-ideal-MHD effects are not essential. In th present model, the physical processes in the inner core are assumed to be the same as in conventional models for the plasmasphere and Region II currents. This region will not be discussed in this paper.

In Fig. 1(a), the thick red lines show the field lines where E_y reverses its sign, indicating a flow reversal. Therefore, these lines separate regions with distinct flow directions and correspond to the separatrix surfaces discussed above. The flow in the region between the inner two dayside red lines expands outward. The

radial velocity at either line is zero and the flow turns to or comes from the azimuthal direction. Similarly, the flow earthward (tailward) of the nightside inner red line contracts inward (expands outward). Therefore, the nightside inner and the dayside middle red lines correspond to surface β. The dayside innermost red line corresponds to surface γ. The nightside branch of surface γ is difficult to resolve in the simulation because of a very low velocity in a very large region. The outermost two red lines correspond to field lines slightly earthward of surface α. Similar patterns can also be found in the results of Usadi et al. (1993), and Fedder and Lyon (1995). In 3-D, surfaces β and γ are similar to the skin of an orange. Surface α has a shape similar to the magnetopause in conventional closed magnetosphere models with one exception: the cusp is not a single point but a spread arc. This spreading is due to the finite width of the reconnection region and the motion of the feet of the magnetospheric boundary layer in the ionosphere.

3.4. Ionospheric mapping

The magnetospheric separatrix surfaces are mapped to the ionosphere along field lines. Since our model is qualitative, the details of a field line model for the mapping is not essential. The separatrix surface between the inner core and the outer magnetosphere (surface γ) is assumed to be the plasmapause which maps (along the magnetic field lines) into the mid-latitude ionosphere. Surface β maps into the equatorward boundary of the polar cap.

The separatrix surface between the boundary layer/tail and the solar wind (surface α) is the magnetopause and it maps into a small arc near the dayside ionospheric cusp (see Fig. 2(c)). In some previous models, the magnetopause maps to a single point at the cusp and in the ionosphere. We think that this single-point mapping has resulted from the static description of the magnetospheric field used in these models. In our model, the magnetopause field lines move continuously along surface α from noon to midnight as shown in Fig. 2(b). They are equipotential. The finite ionospheric conductivity allows a slippage at the feet of the field lines in the ionosphere. Therefore, the cusp spreads into an arc. The length of this arc is determined primarily by the ionospheric resistivity (i.e. the amount of the allowed slippage). In Fig. 1(b), since our software to view the 3-D results is currently limited to the noon–midnight meridian plane, the mapping of surface α from the MHD simulation cannot be shown.

3.5. Magnetospheric convection

The equatorial magnetospheric convection pattern consists of a pair of cells and a pair of channels, one of each on the morning side and the other on the evening side of the noon–midnight meridian, as shown in Fig. 2(b). Connected by the two channels are a dayside source region and a nightside sink region located in the distant tail. The source region (shade region where magnetic flux enters the magnetosphere from the magnetosheath) and the sink region (shaded region where magnetic flux leaves the magnetosphere) are results of the reconnection process described above. The convection in the channels is driven by the pressure gradient arising from the expansion of the newly entered magnetosheath plasma (Song and Russell, 1992; Yang et al., 1994; Song et al., 1994). While flowing in the channels, the plasma undergoes an 'aging' process through microphysical processes (such as the pitch angle diffusion and magnetospheric particle entrainment). Its distribution and composition changes from sheath-like to more magnetospheric (Song and Russell, 1992). It is worth mentioning that near the last closed field line, the plasma velocity is subsonic, shown in both Fedder and Lyon (1995) and our simulation. This is because the plasma is in the closed field line region and the magnetic tension force tends to reduce the flow speed. The downstream sink provides an additional force enhancing the convection. The force is associated with the change in the direction of the magnetic curvature force. For a flux tube, in the magnetosphere, the curvature force is earthward. After being disconnected from the magnetosphere, see the few field lines on the right in Fig. 1(a), the force becomes antisunward as the portion of the flux tube is accelerated to catch up the portions in the solar wind.

The two convection cells are similar to the conventional antisunward convection near the magnetopause boundary and the return flow near the noon–midnight meridian. These cells are driven by ionospheric coupling, the viscous force (e.g., Sonnerup, 1980), and other mechanisms that facilitate mass, momentum and energy transfer across surface β (e.g., Drakou et al., 1994) although only the ionospheric coupling is essential to our model. Point b is where the magnetospheric flow bifurcates either sunward or continuously antisunward, and is crucial to our model.

A major difference between our model and previous viscous interaction models is that, in our model, the viscous interaction is not between the solar wind and the magnetosphere but between the boundary layer plasma and the magnetosphere. It is also important to point out that in our model the electromagnetic coupling between the magnetosphere and the ionosphere acts as a driving force for the convection cells and not as a drag (see more discussion in current systems subsection). We think that such coupling is more effective than the viscous and diffusive interactions alone.

3.6. Ionospheric convection

In our model, to map the equatorial magnetospheric convection to the ionosphere, we use the ideal-MHD assumption. In ideal-MHD, magnetic field lines are equipotentials because the electric field is zero along the field. According to ideal-MHD, the streamlines are also equipotentials because the electric field is zero in the direction of the velocity. Therefore, in the mapping process, neither field linen or streamline will cross each other except at locations where reconnection takes place. Mapping the proposed magnetospheric convection to the ionosphere results in a four-cell convection pattern.

In high latitudes, there are a pair of sunward convection cells with the same polarity as the reverse cells. We will refer to these cells as reverse cells. It is particularly interesting to understand that an ionospheric sunward convection can be caused by a magnetospheric antisunward convection. Let us look at the antisunward flow on the nightside from point b to point a in Fig. 2(b). This convection is from surface β to surface α in the equatorial region. According to ideal-MHD, the field line just outside of surface β will convect antisunward and become the field line on surface α in Fig. 2(a). Following this motion along the two field lines to the ionosphere, in Fig. 2(a) near the Earth, the two field lines switch their positions with respect to the direction of the Sun. The antisunward convection in the equatorial plane near local midnight becomes sunward convection in the ionosphere near local noon. This corresponds to the flow in Fig. 2(c) from point b to point a. Further sunward convection in the ionosphere is directly driven by the reconnection electric field. The reconnection electric field points from dusk to dawn near point X in Fig. 2(a) and maps to the ionosphere in Fig. 2(c). The electric field causes a sunward convection. This process produces a channel flow across the cusp arc, from point a to point A in Fig. 2(c). The flux tube shortening near the high-altitude cusp in Fig. 2(a) produces some additional sunward convection in the ionosphere, from point A to point B in Fig. 2(c), while diverging the flow from local noon.

Sunward from the cusp arc the flow is confined in a narrow region between surfaces α and β. This region maps to the LLBL where the flow is driven by a pressure gradient as discussed above. At the end of this region (point F in Figs. 2(b) and (c)), the flow takes various paths toward point a. Again, note that the tailward flow in the equatorial plane corresponds to a sunward flow in the ionosphere. The ionospheric footprints of these different flow lines form a pair of cells with the same polarity as the reverse cells. The reverse cells are driven by the boundary layer convection and reconnection itself. Because the driving forces are concentrated near points A, F and a, and in the reconnec-tion channel between a and A, it is expected that the reverse cells are centered between A and a, and two Fs. Observations may have shown the indication of such characteristics (Ridley, 1997, private communication). It is also anticipated that the convection in the region antisunward far from the cusp arc should be relatively weak, or even difficult to define observationally.

The magnetospheric convection cells map to a pair of cells in the same sense as viscous cells in the ionosphere. Although we will refer to these cells as viscous cells, as will be discussed in the next subsection, these two cells are not driven by viscous interactions. Instead, they are driven by the ionospheric currents and drive the magnetospheric convection cells. More detailed discussion on this issue will be given in the next subsection.

The two thick red circles in Fig. 1(b) separate the regions of distinct flow directions and correspond to the footprints of surfaces β and γ in Fig. 2(c). The red dot sunward of the pole indicates the location between the footpoints of the two outermost red lines in Fig. 1(a), which are slightly earthward of surface α. Points A and a should be on each side of the center of the dot. We are currently unable to trace the spread of surface α from simulation because of the limitation of the diagnostic programs. The quantitative differences in the ionospheric cells between the model and simulation may also partly be caused by the simplified ionospheric model used in the simulation. We expect that the field-aligned currents and convection are more concentrated on the dayside of the pole than the simulation results, because the real dayside ionospheric conductivity is significantly larger than that on the nightside. The higher conductivity will draw more currents into the dayside region. Since the ionospheric boundary of our MHD simulation model is highly simplified (using a uniform conductivity) and not realistic and our theoretical model is qualitative, they cannot be compared quantitatively. Nevertheless, the four-cell convection pattern is also shown in the simulation of Fedder and Lyon (1995).

3.7. Current systems

The flow in the boundary layer and distant tail results in an increasing tailward distortion of the magnetospheric field. This distortion corresponds to a pair of field-aligned currents mapping to the ionosphere in the same sense as the NBZ currents. The flow reversal regions of the viscous cells correspond to the Region I currents. Ionospheric Pedersen currents connect NBZ and Region I currents in the ionosphere. Fig. 3 demonstrates the electromagnetic coupling at the magnetosphere–ionosphere interface in a northern-hemisphere dawn–dusk cut looking from the Sun. Below
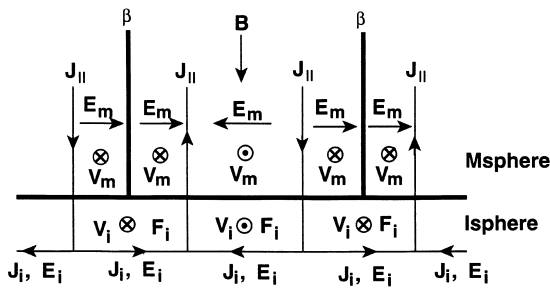
Fig. 3. A dawn–dusk cut of northern-hemisphere ionosphere–magnetosphere interface looking from the Sun. The magnetosphere (ionosphere) is above (below) the thick horizontal line. The magnetic field points downward. The noon–midnight meridian is at the middle of the figure. The footprints of surface β are indicated by the two thick vertical lines. The middle (outer) two field-aligned current $J_{\parallel}$ are the NBZ (Region I) currents. Subscripts 'm' and 'i' denote quantities in the magnetosphere and ionosphere, respectively. V, E, and F are the velocity, electric field and Lorentz force. Note that without the ionospheric coupling, the magnetospheric convection velocities on each side of β have no relationship, but they become coupled with the ionospheric currents which flow beneath the magnetosphere–ionosphere boundary.

the thick horizontal line is the ionosphere, and above it is the magnetosphere. The geomagnetic field points downward. The field-aligned currents $J_{\parallel}$ are generated by or associated with the distortion of the magnetospheric field from a dipole field. The middle pair has the polarity of the NBZ currets and the outer pair, the Region I currents. These currents flow into (out of) the ionosphere and diverge to (converge from) the ionosphere Pedersen currents, J_i. The ionospheric currents generate the ionospheric electric field E_i according to Ohm's law. Within the polar cap, between β, the magnetospheric convection velocity V_m is driven by the magnetospheric motional electric field E_m which can be mapped from the equatorial plane. This magnetospheric convection is directly driven by reconnection at the cusps and the LLBL pressure-driven flow as discussed in the last few subsections. If there is no viscous or diffusive interaction occurring at surface β, the regions equatorward (away from the middle of the figure) of surface β cannot be directly driven by the magnetospheric processes. The concept of the separatrix surfaces is based on ideal-MHD. The footprints of the surfaces end at the interface between the ionosphere and magnetosphere. As the NBZ field-aligned currents penetrate into the ionosphere where collisions are dominant, ideal-MHD does not apply. The Pedersen currents flow beneath the footprints of surface β and couple the energy, in the form of electrical energy, into the regions of 'viscous' cells. Part of the energy dissipates in this region as the Joule heating and the remainder drives the ionospheric 'viscous' cells. The driving force of the ionospheric convection is the Lorentz force F_i as indicated in Fig. 3. The ionospheric convection velocity can be determined according to the electric field drift velocity associated with E_i. This drift velocity is then coupled to the magnetosphere in the regions equatorward of surface β. The magnetospheric electric field E_m, which is directly related to E_i because field lines are equipotentials, then drives the rest of the outer magnetospheric cells.

An interesting point to understand in this process is that the ionosphere, although dissipative, can act as a driver of the magnetospheric convection. There are a few concepts that have been confusing. They are dissipation, generator, driver, driving force, drag and drag force. The ionosphere is dissipative. A dissipative process converts electromagnetic energy into thermal energy and $J \cdot E$ is greater than zero. This definition does not prohibit a dissipative region to act as a driver. A driving force (drag force) is described in the momentum equation when the force is parallel (antiparallel) to the motion direction; namely $F \cdot V$ is greater (less) than zero. If the force is the Lorentz force $J \times B$, the ionosphere $F \cdot V$ has the same sign as $J \cdot E$. Since in the ionosphere $J \cdot E$ is positive, the Lorentz force is always parallel to the motion and is always a driving force of the ionospheric convection. This is quite different from the function of the Lorentz force in the magnetosphere where the Lorentz force is often against the flow. In magnetospheric modeling, the terms 'driver' and 'drag' are often used, in particular when discussing the global coupling, and sometimes they are confused with the terms driving force and drag force. A driver (drag) is the source (sink) of the energy and momentum of the motion. In the case of ideal-MHD, the motion in different parts of a flux tube is linked by the frozen-in condition. Namely, when one part of the flux tube moves, the electric field associated with this motion will couple to the rest of the flux tube and makes the whole flux tube move. The part of the flux tube that generates the original move is the driver of the motion. Another confusion is about the generator. A generator converts plasma thermal or kinetic energy into the electromagnetic energy ($J \cdot E < 0$). When only thermal energy is involved, a generator performs a reverse process of dissipation. It does not specify whether a generator is a driver or drag. As we discussed above, the ionosphere may act as a driver or a drag but never as a generator.

The LLBL/tail region acts as a generator converting the flow energy into the electromagnetic energy. Part of the energy is carried by the field-aligned currents feeding into the ionosphere and drives the ionospheric reverse cells. Therefore, the magnetosphere is the driver of the reverse cells. Separated by surface β, the outer magnetosphere cannot obtain energy directly from the LLBL/tail convection channels if there is no diffusion or viscous interaction. As we discussed above, the Pedersen currents cross surface β from below and couple energy into the 'viscous' cells.

Therefore, the ionosphere is the driver of the outer magnetospheric convection cells. Here we want to point out that a universal simple statement that the ionosphere is a drag can be misleading.

Near the equator, corresponding to the field distortion in the boundary layer/tail, a cross-field current connects the NBZ and Region I currents in the same manner as discussed by Sonnerup (1980) and Song et al. (1994). This connecting current acts to slow down the boundary flow and is an important means to converting the flow energy into the electromagnetic energy, so that it can be coupled to the ionosphere.

4. Discussion

4.1. Energy coupling chain

In our model, viscous and diffusive interactions may play some roles in some regions, such as at each of the separatrix surfaces, but they are not essential to the overall processes. Without considering the effects of viscous and diffusive interactions, the solar wind–magnetosphere–ionosphere energy coupling chain can be described as follows. The solar wind energy through reconnection drives the boundary layer/distant tail convection channels and the sunward flow of the ionospheric reverse cells. The antisunward flow of the ionospheric reverse cells is driven by the boundary layer flow through the electric field coupling. Without viscous and diffusive interaction, the energy cannot directly couple across surface β in the magnetosphere. Namely, the outer magnetosphere convection cells are not directly driven by boundary layer flow. The energy is coupled through the ionosphere. The ionospheric currents couple the energy across surface β below its feet to the ionospheric viscous cells. The ionospheric viscous cells consequently drive the magnetospheric convection cells through the electric field coupling.

4.2. Location of surface β

In ideal-MHD, surface β separates the magnetospheric regions which are directly and indirectly driven by the solar wind. Due to the coupling between the two regions via various mechanisms (such as viscous and diffusive interaction and ionospheric coupling), the convection and magnetic field directions are unchanged across the separatrix surface. However, other plasma properties, such as the density, temperature, and anisotropy, might be different. We think that this surface is located somewhere between the outer and inner parts of the LLBL if the inner edge of the LLBL marks the beginning of the sunward flow.

4.3. Polar cap

If the polar cap is defined as a region in the ionosphere where precipitation particles are observed, the ionospheric footprint of surface β is the equatorward boundary of the polar cap. The polar cap maps to the boundary layer/distant tail region, which contains fresh solar wind plasma. Pitch angle diffusion can scatter these particles into the ionosphere. The region equatorward of the polar cap corresponds to the viscous cells and maps to the outer magnetosphere where the solar wind particles do not have direct access.

4.4. Point b

An important feature of our model is that there is a region in the magnetotail which separates the earthward and tailward flows. In both flow regions, the topology of the magnetic field and plasma characteristics are magnetospheric. We believe that such a feature might have been observed but was difficult to interpret at that time (e.g., Machida, 1996, private communication). The flow velocity at point b is very small. This point is consistent with the flow divergence at -95 Re in Fedder and Lyon (1995) although we do not expect that it is so far from the Earth.

4.5. LLBL formation models

One possible way to place the two existing LLBL models in the present model is the following. The reconnection models and formulations developed by Song and Russell (1992) and Song et al. (1994) are most relevant to the region of the boundary layer in the present model. The viscous interaction models and formulations developed by Sonnerup (1980) and Drakou et al. (1994) are most relevant to surface β.

References

Berchem, J., Raeder, J., Ashour-Abdalla, M., 1995. Reconnection at the magnetospheric boundary: results from global magnetohydrodynamic simulations. In: Song, P., Sonnerup, B.O.U., Thomsen, M.F. (Eds.), AGU Monograph, Physics of the Magnetopause, 90, p. 205.

Burch, J.L., Saflekos, N.A., Gurnett, D.A., Craven, J.D., Frank,

L.A., 1992. The quiet time polar cap: DE 1 observations and conceptual model. J. Geophys. Res. 97, 19,403.

Burke, W.J., Kelley, M.C., Sagalyn, R.C., Smiddy, M., Lai, S.T., 1979. Polar cap electric field structures with a northward interplanetary magnetic field. Geophys. Res. Lett. 6, 21.

Clauer, C.R., Friis-Christensen, E., 1988. High-latitude dayside electric fields and currents during strong northward interplanetary magnetic field: observations and model simulation. J. Geophys. Res. 93, 2749.

Crooker, N.U., 1992. Reverse convection. J. Geophys. Res. 97, 19,363.

Drakou, E., Sonnerup, B.U.O., Lotko, W., 1994. Self-consistent steady state model of the low-latitude boundary layer. J. Geophys. Res. 99, 2351.

Dungey, J.W., 1961. Interplanetary magnetic field and the auroral zones. Phys. Rev. Letts 6, 47.

Fairfield, D.H., 1993. Solar wind control of the distant magnetotail: ISEE 3. J. Geophys. Res. 98, 21,265.

Fairfield, D.H., Lepping, R.P., Frank, L.A., Ackerson, K.L., Paterson, W.R., Kokubun, S., Tamamoto, T., Tsuruda, K., Nakamura, M., 1996. Geotail observations of an unusual magnetotail under very northward IMF conditions. J. Geomagn. Geoelectr. 48, 473.

Feldman, W.C., Hones, E.W., Barraclough, B.L., Reeves, G.D., Belian, R.D., Cayton, T.E., Lee, P., Lepping, R.P., Trombka, J.I., Starr, R., Moersch, J., Squyres, S.W., Rich, F.J., 1995. Possible conjugate reconnection at the high-latitude magnetopause. J. Geophys. Res. 100, 14,913.

Fedder, J.A., Lyon, J.G., 1995. The Earths magnetosphere is 165 Re long: self-consistent current, convection, magnetospheric structure, and process for northward interplanetary magnetic field. J. Geophys. Res. 100, 3623.

Gombosi, T.I., DeZeeuw, D.L., Groth, C.P.T., Powell, K.G., Song, P., 1998. The length of the magnetotail for northward IMF: Results of global 3D MHD simulations, vol. 15, p. 121. In: Chang, T.S. (Ed.), Center for Theoretical Geo/Cosmo Plasma Physics, Cambridge, MA, 1998.

Gosling, J.T., Thomsen, M.F., Barne, S.J., Elphic, R.C., Russell, C.T., 1991. Observations of reconnection of interplanetary and lobe magnetic field lines at the high latitude magnetopause. J. Geophys. Res. 96, 14,097.

Iijima, T., Potemra, T.A., Zanetti, L.J., Bythrow, P.F., 1984. Large-scale Birkeland currents in the dayside polar region during strongly northward IMF: a new Birkeland current system. J. Geophys. Res. 89, 7441.

Kan, J.R., Burke, W.J., 1985. A theoretical model of polar cap auroral arcs. J. Geophys. Res. 90, 4171.

Kessel, R.L., Chen, S.-H., Green, J.L., Fung, S.F., Boardsen, S.A., Tan, L.C., Eastman, T.E., Craven, J.D., Frank, L.A., 1996. Evidence of high-latitude reconnection during northward IMF: Hawkeye observations. Geophys. Res. Lett. 23, 583.

Ogino, T., Walker, R.J., 1984. A magnetohydrodynamic simulation of the bifurcation of tail lobes during intervals with a northward interplanetary magnetic field. Geophys. Res. Lett. 11, 1018.

Potemra, T.A., Zanetti, L.J., Bythrow, P.F., Lui, A.T.Y., Iijima, T., 1984. B_y-dependent convection patterns during northward interplanetary magnetic field. J. Geophys. Res. 89, 9753.

Raeder, J., Walker, R.J., Ashour-Abdalla, M., 1995. The structure of the distant geomagnetic tail during long periods of northward IMF. Geophys. Res. Lett. 22, 349.

Reiff, P.H., Burch, J.L., 1985. IMF B_y-dependent plasma flow and Birkeland currents in the dayside magnetosphere, 2, a global model for northward and southward IMF. J. Geophys. Res. 90, 1595.

Russell, C.T., 1972. The configuration of the magnetosphere. In: Dyer, E.R. (Ed.), Critical Problems of Magnetospheric Physics. National Academy of Sciences, Washington, DC.

Song, P., Russell, C.T., 1992. A model of the formation of the low latitude boundary layer. J. Geophys. Res. 97, 1411.

Song, P., Holzer, T., Russell, C.T., Wang, Z., 1994. Modeling the low latitude boundary layer with reconnection entry. Geophys. Res. Lett. 21, 625.

Sonnerup, B.U.O., 1980. Theory of the low-latitude boundary layer. J. Geophys. Res. 85, 2017.

Taguchi, S., Hoffman, R.A., 1996. Control parameters for polar ionospheric convection patterns during northward interplanetary magnetic field. Geophys. Res. Lett. 23, 637.

Usadi, A., Kageyama, A., Watanabe, K., Sato, T., 1993. A global simulation of the magnetosphere with a long tail: southward and northward interplanetary magnetic field. J. Geophys. Res. 98, 7503.

Winglee, R.M., 1994. Non-MHD influences on the magnetospheric current system. J. Geophys. Res. 99, 13,437.

Wu, C.C., 1985. The effects of northward IMF on the structure of the magnetosphere. Geophys. Res. Lett. 12, 839.

Yang, Y.S., Spiro, R.W., Wolf, R.A., 1994. Generation of region-1 current by magnetospheric pressure gradients. J. Geophys. Res. 94, 223.